Decadal-scale coastal cliff retreat in southern and central California

Adam P. Young[1]

[1] Scripps Institution of Oceanography, University of California San Diego, 9500 Gilman Dr., La Jolla, CA, 92093-0209, USA, adyoung@ucsd.edu

Airborne LiDAR data collected in 1998 and 2009-2010 were used to measure coastal cliff erosion and retreat between the Mexico/California border and Bodega Head, California. Cliff erosion was detected along 44% of the 595 km of shoreline evaluated, while the remaining cliffs were relatively stable. The mean cliff top retreat rate was 0.12 m/yr, while mean retreat averaged over the entire cliff face was 0.04 m/yr. The maximum cliff top and face retreat rates were 4.2 and 3.8 m/yr, respectively. Historical (~1930's to 1998) and recent retreat rates were significantly inversely correlated for areas with large historical or recent cliff retreat, such that locations with elevated historical retreat had low levels of recent retreat and locations with elevated recent retreat were preceded by low rates of historical retreat. The strength of this inverse correlation increased with cliff change magnitudes up to r^2 of 0.91 for cliff top retreat rates greater than 2.9 m/yr. Mean recent retreat rates were 48-74% lower than mean historical retreat rates. Although beaches can protect cliffs against wave-driven erosion, cliffs fronted by beaches retreated 49% more than cliffs without beaches. On average, unarmored cliff faces

retreated 0.05 m/yr between 1998 and 2009-2010, about three times faster than artificially armored cliffs. Alongshore metrics of wave-cliff impact, precipitation, and cliff hardness were generally not well correlated with recent cliff changes. A cliff hazard metric is used to detect cliff steepening and areas prone to future cliff top failures.

Highlights

- Recent decadal-scale cliff retreat is quantified for 595 km of the California coast
- Large magnitude historical and recent cliff retreat rates were inversely correlated
- Cliffs fronted by beaches retreated 49% farther than cliffs without beaches
- Cliff retreat rates are used to detect cliff steepening and areas prone to future cliff top failure

Keywords: coastal cliffs, LiDAR, coastal erosion, California

1. Introduction

Coastal cliffs comprise a high proportion of the world's coasts (Emery and Kuhn, 1982), where almost one quarter of the global population resides (Small and Nicholls, 2003). Retreating coastal cliffs currently cause numerous problems for coastal populations and managers. Sea-level rise is expected to cause increased coastal cliff erosion rates for many areas (Sunamura 1988; Bray and Hooke, 1997; Dickson et al., 2007; Nicholls et al., 2007; Trenhaile, 2010; 2014). Studies of coastal cliff erosion and retreat have increased in recent years (Naylor et al., 2010), highlighting a growing interest and need to study rock coasts. Yet our understanding of coastal cliff processes and behavior is complicated by the wide array of erosional processes that occur (Trenhaile, 1987; Sunamura, 1992; Rosser et al., 2007; Kennedy et al., 2011), variable temporal changes and processes (Cambers, 1976; Dornbusch et al., 2008; Lee, 2008), geomorphic feedbacks (Sunamura, 1976; Kline et al., 2014; Young, 2015), and highly variable geologic, oceanographic, and climatic settings.

Actively eroding coastal cliffs comprise the majority of the California coast (Fig. 1) and threaten development throughout the State, including highways, railways, wastewater, oil, natural gas and nuclear facilities, universities, military bases, and numerous state beaches and parks in addition to homes and businesses. Episodic

cliff failures have caused human injury and several deaths in recent years (*e.g.* Perry, 2000; Gross and Davis, 2008; Evans, 2015). Seawalls and rock armoring are increasingly used to prevent erosion, but eroding coarse-grained coastal cliffs can be an important source of sediment to beaches (Young and Ashford, 2006; Brooks and Spencer, 2010; Young et al., 2010a; Mushkin et al., 2016), which are important cultural and economic resources that generate billions of dollars annually in California. These problems will worsen as sea levels and coastal populations continue to increase, and effectively managing California's changing coast will become increasingly challenging.

Coastal cliff erosion is broadly attributed to marine and subaerial (including subsurface) erosion mechanisms (Trenhaile, 1987; Sunamura, 1992). Subaerial mechanisms (*e.g.* groundwater processes, rilling, slope wash) act over the entire cliff face, and beneath the surface. Rainfall has been empirically linked to inland landsliding (Caine, 1980), where marine processes are not active, and serves as an indicator of subaerial forcing. Young et al. (2009b) found a high correlation between the timing of rainfall and coastal cliff erosion in southern California. Brooks et al. (2012) discussed the importance of the sequence of rain events on sub-surface pore water pressures and cliff stability. Marine processes (*e.g.* wave-driven impact pressures and abrasion) act directly only at the cliff base, and only when tides and other water level fluctuations allow waves to reach the cliff (Sunamura, 1992; Rosser et al., 2013; Vann Jones et al., 2015; Young et al., 2016). While marine and subaerial processes drive cliff erosion, geologic conditions dictate cliff resistance

and control the seacliff failure mode. The relative importance of marine and subaerial processes varies in space and time, and observations of cliff erosion and forcing (*e.g.* ocean waves and rain) are needed to establish these relationships. Brooks et al. (2012) established both marine and subaerial process thresholds associated with high magnitude cliff retreat events for soft cliffs on the Suffolk coast, U.K. and concluded the driving mechanisms vary through time.

Historical cliff retreat has been measured with historical maps and aerial photographs in a variety of locations worldwide, including Portugal (Marques, 2008), the United Kingdom (May and Heeps, 1985; Brooks and Spencer, 2010), Italy (Budetta et al., 2000), Australia (Bezore et al., 2016), Canada (Lantuit and Pollard, 2008), and India (Sajinkumar et al., 2016). LiDAR is increasingly used to measure more recent cliff retreat and erosion and has been applied in the United Kingdom (Adams and Chandler, 2002; Rosser et al., 2005; Earlie et al., 2014), Portugal (Nunes et al., 2011), the United States (*e.g.* Sallenger et al., 2002; Young and Ashford, 2006), Canada (Obu et al., 2016), Israel (Katz and Mushkin, 2013) and France (Letortu et al., 2015). Other methods to measure cliff retreat and erosion include using fixed markers in the United Kingdom (Williams and Davies, 1987), field surveys in Australia (Gill, 1973), micro-erosion meters (MEM) in New Zealand (Stephenson and Kirk, 1996) and measuring shore platform widths in New Zealand (de Lange and Moon, 2005).

Coastal cliff retreat studies in California date back at least to 1932 (Vaughan, 1932). Since then, numerous studies of California cliff retreat have been conducted using a variety of measurement techniques ranging from dated inscriptions (Emery and Kuhn, 1980) to terrestrial LiDAR (Collins and Sitar, 2008). These studies are often site-specific or local in scale, but Griggs et al. (2005) and Dare (2005) provide statewide compilations of many of these studies, and USACOE (1971) provides a qualitative statewide erosion assessment. Hapke et al. (2009) conducted the most recent systematic study and mapped retreat along 350 km of California cliffs using T-sheets from the 1920s and 1930s and airborne LiDAR data collected in 1998 and 2002. Using shore-normal transects spaced 20 m alongshore, Hapke et al. (2009) calculated mean and maximum cliff top retreat rates of 0.3 m/yr and 3.1 m/yr, respectively, with estimated errors of 0.2 m/yr. The highest retreat rates were in central and northern California, associated with large slumps and deep-seated coastal landslide activity, often triggered by elevated rainfall and associated increased pore water pressures (Thomas and Loague, 2014; Young, 2015).

Advances in cliff mapping with airborne LiDAR surveys (Matsumoto et al., 2017) provide unprecedented detail of volumetric and cliff top change over large areas, but existing studies in California have limited spatial extent (*i.e.* Young et al., 2009a; 2010b; 2011). This study provides the first large-scale assessment of coastal cliff erosion and retreat in California using high-resolution airborne LiDAR data collected in 1998 and 2009-2010. Both cliff top retreat and the average retreat of over the cliff face are quantified and used to explore changes on different parts of

the cliff profile. The results are compared with historical retreat rates, alongshore metrics of erosion forcing mechanisms, and rock strength. A cliff hazard metric described by Young et al. (2009a) is used to locate areas prone to future cliff top failures.

2. Study Site

2.1. Geologic Setting

The study site extends 1100 km from the Mexico/California border to Bodega Head, California (Fig. 1). The California coast is tectonically active and contains numerous fault zones, most notably the San Andreas Fault dividing the North American and Pacific plates. Past tectonic processes produced several coastal mountain ranges and a series of uplifted marine terraces along much of the coastline. The majority of coastal cliffs are low relief cliffs cut into the uplifted marine terraces while the rest are high relief cliffs and coastal mountains (Griggs et al., 2005).

Cliffs cut into the marine terraces are generally composite cliffs composed of two geologic units: a more resistant lithified Cenozoic mudstone, shale, sandstone and siltstone, and an upper unit of weakly lithified Quaternary terrace deposits (Griggs et al. 2005). Low-relief cliffs composed of alluvium or terrace deposits also exist where the lower unit is locally absent. The cliffs are generally 10–30 m in height, but

exceed 100 m in some areas. Cliff heights remain generally constant as the cliff recedes because most cliff tops are relatively flat terrace features. The cliffs are typically fronted by a wave-cut platform usually covered by a veneer of beach sand and sometimes cobble. The beaches, which act as a buffer to direct wave-driven cliff erosion, are often narrow and occasionally stripped of sediment during large winter storms. Cliff profiles differ alongshore and their geometries are related to the relative importance of marine and subaerial processes, cliff composition, and phases of cliff profile evolution (Emery and Kuhn, 1982).

2.2. Oceanography

The California coast is exposed to waves generated by local winds and distant storms in both hemispheres (Flick, 1994). During winter, swell from the North Pacific and Gulf of Alaska is most energetic, whereas swell from the South Pacific dominates in summer. Waves reaching the southern California coast undergo a complex transformation, and shadows of the Channel Islands create strong alongshore variations in wave height (Pawka, 1983). Annual nearshore wave energies are generally larger in central (defined here as Point Conception to Bodega Head) and northern California compared to southern California (south of Point Conception). The tide range reaches up to 2.6 m during spring tides, so large swells arriving during relatively low tide may not reach the cliffs, whereas moderate swell arriving during high tide can have significant wave-cliff impact duration (Young et al., 2016).

2.3. Climate

The climate is characterized by dry summers and occasionally wet winters, with most rainfall occurring from November to March. Prolonged drought, very wet years, and multi-decadal scale precipitation cycles can cause high variation in annual rainfall (Michaelsen et al., 1987; Haston and Michaelsen, 1994). Annual coastal precipitation generally increases northward with mean annual precipitation ranging from 257 mm in San Diego to 1032 mm near Bodega Head (www.wrcc.dri.edu), but is locally higher along the Big Sur coast and lower in the San Francisco and Monterey areas. Strong El Niño events are usually associated with elevated winter precipitation, wave heights, and sea levels, causing increased coastal erosion, flooding and damage (Flick 1998; Storlazzi and Griggs 2000; Storlazzi et al., 2000; Barnard et al., 2017). Annual precipitation during the study was near average except during the winter of 2004-2005 when some regions received more than twice the annual mean precipitation.

3. Methods

3.1. LiDAR data

Airborne LiDAR datasets collected in 1998 and 2009-2010 (coast.noaa.gov/digitalcoast/; Table 1) provide regional coverage from the

California-Mexico border to Bodega Head, with some gaps, notably along the Big Sur Coast (Fig. 1). A 2002 LiDAR dataset provides additional spatial coverage but was not used here because of low point density (probably from fewer aircraft flight passes) and data gaps. However, a cliff top line digitized by Hapke and Reid (2007) from the 2002 LiDAR was used in some localized areas. The overall coverage for this study includes 595 km of cliffs.

The LiDAR survey contractors estimated vertical root mean square error of the 1998 and 2009-2010 point data at 0.15 m, with horizontal accuracies of 0.5-0.80 m. LiDAR point data were processed into 1-m resolution digital elevation models using the last return (if multiple returns were available) and a natural neighbors technique. Typical point density of the 1998 and 2009-2010 datasets are 0.5 and 1.5 points/m^2, respectively.

3.2. Cliff erosion and cliff face retreat (1998 to 2009-2010)

Digital change grids, estimated by differencing successive digital elevation models created using these LiDAR datasets, show both negative (erosion) and positive (accretion, talus deposits) changes. Sources of digital change grid error include the basic LiDAR observations, spatial interpolation, and vegetation. The vertical root mean square difference (RMSZ) between surveys was estimated at 0.36 m using 14 control areas spread throughout the study area. Control areas representative of coastal cliff topography consisted of inland hillsides and slopes assumed to

experience no change during the study period. RMSZ was calculated for each control area using the digital change grid raster values.

Elevation changes can indicate landslide motion, land erosion, talus deposition, topographic beach changes, and anthropogenic changes. The detected changes were programmatically filtered to remove noise and erroneous data. To do so, first all grid cells with a vertical change of less than 1 m (about 3 * RMSZ) were omitted. Next, a minimum topographic footprint was imposed, requiring more than 10 connected cells of positive or negative change. Finally, the filtered digital change data were checked visually and edited manually. Changes related to beaches, dunes, construction, and those areas inland of the coastal road were identified using aerial photographs and digital elevation model hillshades, and removed.

Changes were separated into negative (*i.e.* cliff erosion) and positive (*i.e.* talus deposits) volumetric changes and then evaluated in 5 m wide (in the alongshore direction) compartments. Dividing the volumetric compartment changes by the cliff height and compartment width (5 m) yielded bulk negative and positive cliff face changes, equivalent to average cliff retreat/advance over the cliff face (Fig. 2). Cliff/coastal slope heights were obtained from the digital elevation model.

The calculated volume changes under-estimate the actual changes because only relatively large volume and large footprint slides are detected. Thus, smaller topographic changes (such as a smaller individual rockfalls or localized surficial

erosion) were not detected with the present methods. In a few locations such as Palos Verdes and Big Sur, the LiDAR swath did not fully cover the landward extent of coastal change, also causing an under-estimation of coastal change volumes.

3.2. Cliff top retreat (1998/2002 to 2009-2010)

Cliff top changes were measured using an existing 1998 (or 2002 in some locations) cliff top edge line from Hapke et al. (2007) and a 2009-2010 cliff top edge line digitized manually for this study. The cliff top edge location was defined as the slope break between the cliff face and the cliff top. Areas were excluded where a definitive edge could not be identified. Cliff top retreat was measured at 5 m intervals alongshore using shore-normal transects. Negative cliff top retreat indicates landward cliff top movement (erosion). Measurements indicating seaward cliff top movement were assumed to result from data processing artifacts, and set to 'no change'. In some localized areas, cliff top retreat measurements were removed because of variation in the identified cliff top edge feature between this study and Hapke and Reid (2007). Cliff edge uncertainties of 1.3 and 1.1 m for the 1998 and 2009-2010 datasets, respectively, were estimated as the sum in quadrature of the horizontal LiDAR accuracy (0.5 and 0.8 m) and digitizing error estimated at 1 m. The annualized error for cliff top retreat rates was estimated as the sum in quadrature of the two cliff edge uncertainties divided by the time span (11.6-12.4 years) at 0.14-0.15 cm/yr.

3.3. Historical cliff top retreat (1929-1934 to 1998/2002)

Historical cliff edge lines from 1929-1934 and 1998/2002 (previously analyzed by Hapke and Reid, 2007) were reanalyzed at 5 m alongshore resolution for spatial consistency with the present analysis. Measurements indicating seaward cliff top movement were set to 'no change'. The error associated with these cliff retreat rates is estimated at 0.20 m/yr (Hapke and Reid, 2007).

3.4. Waves and Total Water Level

Hourly tide levels were obtained from the La Jolla, Los Angeles, Santa Monica, Santa Barbara, Port San Luis, Monterey, and Point Reyes tide gauges (tidesandcurrents.noaa.gov). A wave buoy network (CDIP, cdip.ucsd.edu) was used to estimate hourly wave conditions at 8707 virtual buoys located in 10 m water depth spaced at 100 m intervals alongshore. The effects of complex bathymetry, and of varying beach orientation and wave exposure, were simulated with a spectral refraction wave model initialized with offshore buoy data (O'Reilly and Guza, 1991; 1998). The model has been used throughout California and validated extensively (O'Reilly et al., 2016). Time periods without data at all virtual buoys were removed, resulting in 46,258 hours between November 2003 and November 2009 for wave data analysis.

The total water level is the sum of tides and the vertical height of wave run-up (Shih et al., 1994; Kirk et al., 2000; Ruggiero et al., 2001). Time series of hourly total water level at the cliff base provide basic estimates of wave impact duration and a proxy for marine forcing. The vertical height of wave run-up (R2%) was approximated as the level exceeded by 2% of wave uprushes (Stockdon et al., 2006), using the formula:

$$R2\% = 0.043(H_o L_o)^{0.5}$$

where the deep water wave height (H_o) used in the run-up equation was calculated by backing out nearshore wave height to deep water by reverse shoaling using linear wave theory, while the deep water wavelength (L_o) was calculated using the linear dispersion relationship (Dean and Dalrymple, 1991). Hourly total water level at each cliff location was interpolated with R2% and tide gauge data and used to calculate wave-cliff impact metrics, defined as the number of hours total water levels exceeded 2.5 and 3 m in elevation (NAVD88).

3.5. Coastal Armoring and Setting

Coastal armoring present in 2010 was mapped by updating and amending a 2004 database of coastal armoring (Dare, 2005) using 2010 oblique coastal photographs (California Coastal Records Project). The general coastal setting (rocky coast, sandy beach, cliff fronted by beach, etc.) was categorized and mapped alongshore using

maps from Griggs et al. (2005) and 2010 oblique photographs (California Coastal Records Project). An accurate time series of beach width could not be established for the study area because of limited data availability and variable survey dates (Table 1) combined with large seasonal beach fluctuations, sometimes more than 50 m (Doria, 2016).

3.6. Rock Strength

Nine hundred and thirty three *in situ* cliff rock strength measurements were made with Proceq Schmidt Hammers Type L and N at the cliff base using the ASTM method (ASTM, 2013). The ASTM method calculates the rebound value as the mean of 10 readings with outliers removed. Type L and N hammers were compared using 20 *in situ* measurements on a variety of rock types and combined with measurements from Kennedy and Dickson (2006) for calibration. Type L and N measurements were highly correlated ($r^2 = 0.98$), and Type N hammer measurements were converted to Type L for consistency. Schmidt hammer measurements were typically spaced 50-100 m alongshore in the sections evaluated. For each cliff compartment rebound measurements located within 100 m were used to evaluate rock rebound statistics including the minimum, maximum, mean, and non-zero mean. Similar rock rebound metrics were also evaluated using rebound measurements within 500 and 1000 m of each cliff compartment. Site access logistics limited most rock strength measurements to cliffs fronted by beaches.

3.7. Precipitation

Total precipitation during the study period was estimated by interpolating daily precipitation records from 18 coastal sites distributed over the study area to each 5 m alongshore compartment (Fig. 1; www.wrcc.dri.edu/).

3.8. Cliff Top Hazard Index

Over long periods, cliff face and cliff top retreat measurements will converge. However over shorter time periods, these measures can differ substantially and provide information on geomorphic change and cliff stability. Cliff top retreat reduces the overall cliff slope, while cliff base and cliff face erosion (not concentrated at the cliff top) cause slope steepening, thus reducing overall cliff stability. Young et al. (2009a) suggested the difference between cliff top and cliff face erosion could be used as a cliff top retreat hazard index. For example, as the cliff face retreat exceeds cliff top retreat, the cliff becomes more unstable, and vice versa. A cliff top hazard index, defined here as the recent cliff top retreat rate (positive values set to zero) minus the recent cliff face net retreat, increases with overall cliff steepening. Positive hazard values indicate the cliff face retreat rates exceed the cliff top retreat rates, suggesting a higher potential for future cliff top failure.

4. Results

4.1 Coastal Setting

Seventy percent of the studied shoreline contains coastal cliffs, with 57% fronted by beaches (Fig. 3a, Table 2). Beaches without cliffs occupy 27% of the shoreline, with the remaining 3% of the coastline consisting of harbors and waterways. Total water level index metrics were consistently higher north of Point Conception (Fig. 3c). Eighteen percent of alongshore compartments contained some level of coastal armoring (Fig. 3a). Armoring is more prevalent in southern California probably because of higher density coastal populations and development, despite lower nearshore wave energies. Rock rebound values were relatively low in the San Diego area (Table 2), but generally varied widely in the sampled areas (Fig. 3e).

4.2. Cliff Changes

Recent (1998 to 2009-2010) cliff changes greater than 10 m^3/yr were detected in 44% of the 5 m alongshore compartments (267 of 595 km; Table 3, Fig. 4d). Recent net volumetric cliff change rates ranged from -527 (erosion) to 128 (accretion) m^3/m/yr with a mean of -1.78 m^3/m/yr (Table 3). Recent net cliff face retreat ranged from -3.8 (landward) to 0.67 (seaward) m/yr with a mean of -0.042 m/yr (Table 3, Fig. 4c). Recent cliff top retreat rates ranged from -4.2 to 0.0 m/yr, with a mean of -0.12 m/yr (Table 3, Fig. 4b) for the 236 km evaluated. In comparison, historical (1929-1934 to 1998/2002) cliff top retreat rates ranged from -3.1 to 0.0

m/yr, with a mean of -0.25 m/yr (Table 3, Fig. 4a) for the 283 km evaluated. Across the 169 km of cliffs where both historical and recent cliff top rates exist, the mean historical and recent cliff top retreat rates were -0.22 and -0.12 m/yr, respectively

Numerous cliff erosion and retreat hot spots were detected throughout the study area (Fig. 5). Many of the erosion hot spots were related to deep-seated and/or complex coastal landslides such as in Daly City, Portuguese Bend, and San Onofre, consistent with previous studies (Hapke et al., 2009, Young et al., 2009b; Young, 2015).

4.3. Cliff Top Hazard Index

The cliff top hazard index ranged from -3.7 to 1.7 (Fig. 4e) with a mean of -0.07, indicating more areas experienced cliff flattening as opposed to cliff steepening. However, 33% of compartments with both cliff top retreat and cliff face retreat observations had a positive hazard index. Locations with large cliff top hazard values (> 1) include San Onofre State Beach, Big Sur, Martin's Beach, Daly City, and near Double Point in Point Reyes National Seashore. San Luis Obispo County had the highest overall mean hazard index but the mean index of cliff steeping locations (positive hazard values) was relatively low (Table 2). Marin, San Francisco, and San Mateo Counties, all in the northern part of the study area, had the highest mean index of cliff steepening locations. Marin, San Luis Obispo, and Santa Barbara Counties had the highest percentages (42-62 %) of cliff steepening locations (Table

2). Additional future surveys are needed to test the applicability of this experimental hazard index.

5. Discussion

5.1. Influence of Coastal Setting

Correlations between total water level metrics and recent cliff changes were not significant at spatial scales between 5 m – 0.5 km (averaging alongshore), but became statistically significant ($p<0.01$) at 0.5 km scale, and increased to a maximum of ~0.15 (r^2) at 15 km scales. At larger scales, the correlations became unstable with high r^2 fluctuations. Although not available for this study, incorporating time series data of beach widths and elevations to assess wave-cliff impacts may improve correlations between marine forcing and cliff retreat. Neither precipitation nor rock rebound metrics were well correlated with cliff retreat at any spatial scales. This could be because of the relatively low sampling resolution for rainfall and rock strength compared with cliff changes, or that other local parameters such as sea spray, wind, and beach elevations are influencing cliff retreat. For example, rainfall runoff directed onto specific cliff areas can create erosion hot spots unrelated to cliff hardness or regional rainfall quantities. Additionally, the decadal time span averages out high magnitude rain and wave events causing the cliff erosion. The processes driving cliff erosion vary in space and time, and alongshore differences in cliff stage profile development and the

stochastic nature of cliff failures probably also limited cliff erosion correlations. As identified in previous work (*e.g.* Young et al., 2009b; Young 2015), rainfall may be better correlated with cliff erosion when compared in time series rather than the spatial comparison used here because time series analysis of a particular cliff section reduces cliff setting variables (such as geologic conditions) that are difficult to quantify.

Mean cliff face and cliff top retreat rates in central California were 86% and 30% larger, respectively, compared to southern California. Similarly, mean metrics of wave-impact and precipitation were also higher in central California, suggesting possible relationships at these regional scales; however additional data are needed to test this relationship statistically.

On average, unarmored cliffs retreated (-0.054 m/yr cliff face retreat) about 3 times more than armored cliffs (-0.019 m/yr, Fig. 6a). Cliffs fronted by beaches retreated 49% more (-0.061 m/yr cliff face retreat) than those without beaches (-0.041 m/yr, Fig. 6a). This observation is counter-intuitive because beaches protect cliffs from wave erosion (Jones and Williams, 1991; Lee, 2008), but is consistent with previous studies (Robinson, 1977). This observation suggests beaches in the study area tend to form at locations with relatively weak cliffs and where sufficient sand supply exists. It also highlights the possible role of beach sediment as an abrasive that may accelerate cliff retreat (Sunamura, 1982; 1992; Kline et al., 2014). Additional rock strength sampling at sites without beaches, and an evaluation of the beach

protective capacity may help test this hypothesis. It is unknown if this relationship will hold over longer time periods, however it is consistent with long-term modeling (Limber et al., 2014; Limber and Murray, 2014) suggesting beaches accumulate in embayments composed of weak rock. This finding is also consistent with wave refraction around headlands that generate gradients in alongshore sediment flux and sediment deposition in embayments (May and Tanner, 1973; Komar, 1985; Carter et al., 1990; Trenhaile, 2016).

Taller cliffs experienced more overall erosion (Fig. 6c), but cliff face retreat rates were generally uninfluenced by cliff height except for low height cliffs (0-10 m) that retreated slower than all other cliffs (Fig. 6b). The reason for the small retreat rates of low cliffs is unknown, but could be from erosion-resistant low cliffs that sometimes lack the weaker upper Quaternary layer (for example in the Monterey area). At 5 m compartment scale, cliff height was not correlated with recent cliff retreat or erosion. However when retreat rates from unarmored cliffs were binned by height (10 m bins), the mean cliff height for each bin was significantly correlated with mean erosion rate when bins with fewer than 1000 observations were excluded ($r^2 = 0.71$, Fig. 6c). This correlation between mean binned cliff retreat rates and unarmored cliff height decreased when bins with fewer observations were considered.

5.2. Comparison to Historical Retreat Rates

Distributions of historical and recent retreat rates were all skewed towards smaller magnitude events, but historical retreat rates were more evenly distributed and included higher percentages of large magnitude retreat rates (Fig. 7). The more evenly distributed historical cliff retreat could be because longer time periods average out the stochastic nature of cliff retreat, and suggests the system moves towards more spatially uniform retreat rates with time. One percent of historical cliff top, recent cliff top, and recent cliff face retreat rates exceeded -1.0, 0.6, and 0.35 m/yr, respectively. Mean recent cliff top and cliff face retreat rates were lower than mean historical cliff top retreat rates by 48% and 74%, respectively (mean rates include zero change locations). The reason for the substantially lower rates is unknown but could be related to extensive anthropogenic alterations to the coastal system, different overall time scales (~70 vs. ~10 years), the episodic nature of cliff retreat, changes in ocean or subaerial forcing between these time periods, and/or variable quality of data sources. Additional retreat measurements over a wider variety of timescales are needed to test for timescale-dependence of erosion rates observed in other natural systems with intermittent erosion events (e.g. Finnegan et al., 2014; Ganti et al., 2016). However, in these other systems erosion rates are higher over shorter time intervals, opposite to the smaller decadal scale rates observed here. This opposition could be from the large spatial area evaluated here that can reduce the timescale-dependence of erosion rates (Sadler and Jerolmack, 2014; Ganti et al., 2016). Historical and recent maximum retreat rates were of similar magnitude.

Overall comparison of historical and recent individual compartment retreat rates (Fig. 8a, 8b) suggests they are not well correlated. However, historical and recent retreat rates are significantly ($p<0.01$) inversely correlated for areas that experienced relatively large historical or recent cliff retreat, such that recent retreat rate decreases with elevated historical retreat. The strength of the inverse correlation increases with cliff change magnitudes up to $r^2 = 0.91$ (Fig. 8d, 8e). This result suggests that using site-specific historical retreat rates to predict or project future decadal scale cliff retreat (and possibly longer time scales) using historical data could be problematic because of the varying timescales, forcing mechanisms, and system feedbacks. The stochastic nature of cliff retreat also complicates predictions when time scales vary and the time elapsed since previous failures is not considered. The inverse correlation is probably driven by geomorphic feedbacks, such that after a large cliff top failure, the cliff becomes relatively inactive from (1) a decrease in cliff slope and (2) increased wave protection from talus (and resulting beaches, when the cliffs contain sufficient beach-size sediment). These findings are consistent with Lee (2008) who found that extrapolating historical retreat is problematic without incorporating cliff-beach dynamics and forcing mechanisms over the observation period.

6. Summary

LiDAR data collected in 1998 and 2009-2010 were used to measure decadal scale coastal cliff erosion and cliff top retreat from the Mexico/California border to Bodega Head, California. Cliff face erosion was detected along 44% of the 595 km of cliffs evaluated. Mean cliff face and cliff top retreat rates were -0.04 and -0.12 m/yr, respectively, notably lower than historical (1929-1934 to 1998/2002) retreat rates of -0.25 m/yr. The lower recent rates could be from anthropogenic changes, varying time periods and forcing mechanisms, the stochastic nature of cliff retreat, and variable quality data sources. Distributions of historical retreat rates were spread more evenly and included higher percentages of large magnitude retreat rates, probably because the longer time span captured more locations that experienced episodic large cliff retreat events, thus spatially averaging out retreat rates. Large magnitude historical cliff retreat rates were inversely correlated with recent cliff retreat rates, suggesting possible problems with using historical retreat rates to project future cliff positions. The inverse correlation is probably driven by the episodic nature of large cliff retreat events, geomorphic feedbacks, and the cliff retreat cycle.

Maximum landward cliff top and cliff face retreat rates were about 4 m/yr, similar to maximum historical retreat rates. Localized high rates of coastal cliff change were found in Palos Verdes, Daly City, San Onofre State Beach, Point Reyes National Seashore, and Martin's Beach and were often related to deep-seated and/or complex coastal landslides. Alongshore metrics of wave-cliff impact, precipitation, and cliff hardness generally did not correlate well with recent cliff retreat rates. On average,

unarmored cliff faces retreated about three times further than armored cliffs. Although beaches can prevent wave-driven erosion, cliffs fronted by beaches retreated faster than those without beaches. However, the influence of beach width was not considered here, and narrow beaches that provide little erosion protection might have influenced this outcome. These findings highlight the need to monitor beach and cliff changes concurrently and examine the protective role of beaches in cliff processes and wave-cliff interaction.

The difference between cliff face change and cliff top retreat were used to quantify cliff steeping and establish a cliff top hazard index. Locations with relatively large cliff steeping and cliff top hazard values include San Onofre State Beach, Big Sur, Martin's Beach, Daly City, and near Double Point. Additional surveys are needed to test the hazard index and identify hazard thresholds and probable timing of future failures.

7. Acknowledgments

APY was funded by the California SeaGrant and California Department of Parks and Recreation, Division of Boating and Waterways (DPR-DBW) with the University of California. Wave data was sponsored by the California DPR-DBW with the University of California and USACE, as part of the Coastal Data Information Program (CDIP). Patrick Limber at USGS graciously provided about 200 Schmidt Hammer rebound observations north of Point Conception. Lucian Parry conducted parts of the GIS

analysis. Jessica Carilli provided thoughtful editing and assisted with Schmidt Hammer field measurements. Bob Guza and Ron Flick provided important support for this research.

8. References

Adams, J., Chandler, J., 2002. Evaluation of LIDAR and medium scale photogrammetry for detecting soft- cliff coastal change. *The Photogrammetric Record*, *17*(99), 405-418.

ASTM, 2013. C805/C805M-13a Standard Test Method for Rebound Number of Hardened Concrete, ASTM International, West Conshohocken, PA.

Barnard, P.L., Hoover, D., Hubbard, D.M., Snyder, A., Ludka, B.C., Allan, J., Kaminsky, G.M., Ruggiero, P., Gallien, T.W., Gabel, L., McCandless, D., 2017. Extreme oceanographic forcing and coastal response due to the 2015–2016 El Niño. *Nature Communications*, *8*, p.14365.

Bezore, R., Kennedy, D.M. and Ierodiaconou, D., 2016. The drowned Apostles: the longevity of Sea stacks over Eustatic cycles. *Journal of Coastal Research*, *75*(sp1), 592-596.

Bray, M.J. and Hooke, J.M., 1997. Prediction of soft-cliff retreat with accelerating sea-level rise. *Journal of Coastal Research*, 453-467.

Brooks, S.M., Spencer, T. and Boreham, S., 2012. Deriving mechanisms and thresholds for cliff retreat in soft-rock cliffs under changing climates: Rapidly retreating cliffs of the Suffolk coast, UK. *Geomorphology*, *153*, 48-60.

Caine, N., 1980. The rainfall intensity duration control of shallow landslides and debris
flows. *Geografiska Annaler*, 62A , 23–27.

Cambers, G., 1976. Temporal scales in coastal erosion systems. *Transactions of the Institute of British Geographers*, 246-256.

Carter, R.W.G., Jennings, S.C., Orford, J.D., 1990. Headland erosion by waves. Journal of Coastal Research 6, 517-529.

Collins, B.D., Sitar, N., 2008. Processes of coastal bluff erosion in weakly lithified sands, Pacifica, California, USA. *Geomorphology*, *97*(3), 483-501.

Dare, J., 2005. Coastal erosion armoring shapefile, https://catalog.data.gov/dataset, California Coastal Commission.

Dean, R., Dalrymple, R., 1991. Water Wave Mechanics for Engineers and Scientists, Advanced Series on Ocean Engineering. World Scientific.

Dickson, M.E., Walkden, M.J. and Hall, J.W., 2007. Systemic impacts of climate change on an eroding coastal region over the twenty-first century. *Climatic change*, *84*(2), 141-166.

Doria, A., 2016. Observations and Modeling of Southern California Beach Sand Level Changes, Ph.D. Dissertation, University of California San Diego, U.S.A.

Dornbusch, U., Robinson, D.A., Moses, C.A. and Williams, R.B., 2008. Temporal and spatial variations of chalk cliff retreat in East Sussex, 1873 to 2001. *Marine Geology*, *249*(3), 271-282.

Earlie, C.S., Masselink, G., Russell, P.E., Shail, R.K., 2015. Application of airborne LiDAR to investigate rates of recession in rocky coast environments. *Journal of coastal conservation*, *19*(6), 831.

Emery, K.O., Kuhn, G.G., 1980. Erosion of rock shores at La Jolla, CA. *Marine Geology,* 37, 197-208.

Emery, K.O., Kuhn, G.G., 1982. Sea cliffs: their processes, profiles, and classification. *Geological Society of America Bulletin*, *93*(7), 644-654.

Evans, B., 2015, Mar 26. Woman dies in bluff collapse at Arch Rock, *Point Reyes Light.*

Finnegan, N.J., Schumer, R., Finnegan, S., 2014. A signature of transience in bedrock river incision rates over timescales of 10^ sup 4^-10^ sup 7^ years. *Nature*, *505*(7483), 391.

Flick, R.E., 1994. Shoreline Erosion Assessment and Atlas of the San Diego Region. Sacramento, California: California Department of Boating and Waterways, 2 volumes.

Flick, R.E., 1998. Comparison of California tides, storm surges, and mean sea level during the El Niño winters of 1982-83 and 1997-98. *Shore & Beach*, *66*(3), 7-11.

Fugro, 2011. Aerial acquisition report for California coastal lidar, Coastal Services Center, NOAA, U.S. Department of Commerce. 56p.

Ganti, V., von Hagke, C., Scherler, D., Lamb, M.P., Fischer, W.W., Avouac, J.P., 2016. Time scale bias in erosion rates of glaciated landscapes. *Science advances*, *2*(10), e1600204.

Griggs, G., Patsch, K., Savoy, L., 2005. Living with the Changing California Coast. University of California Press, Berkeley, California. 540p.

Gross, G. and Davis, K., 2008, August 21. Beach-goer dies after cliff collapses, *The San Diego Union Tribune*.

Hapke, C.J., Reid, D., 2007. National Assessment of Shoreline Change, Part 4: Historical Coastal Cliff Retreat along the CA Coast, USGS Report 2007-1133.

Hapke, C.J., Reid, D., Richmond, B., 2009. Rates and trends of coastal change in California and the regional behavior of the beach and cliff system. *Journal of Coastal Research*, *25*(3), 603-615.

Haston, L, Michaelsen, J., 1994. Long-term central coastal California precipitation variability and relationships to El Niño-Southern Oscillation. *Journal of Climate*, *7*(9), 1373-1387.

Jones, D.G., Williams, A.T., 1991. Statistical analysis of factors influencing cliff erosion along a section of the west Wales coast, U.K., *Earth Surface Processes and Landforms*, 16, 95–111.

Katz, O. and Mushkin, A., 2013. Characteristics of sea-cliff erosion induced by a strong winter storm in the eastern Mediterranean. *Quaternary Research*, *80*(1), 20-32.

Kennedy, D.M., Dickson, M.E., 2006. Lithological control on the elevation of shore platforms in a microtidal setting. *Earth Surface Processes and Landforms*, *31*(12), 1575-1584.

Kirk, R.M., Komar, P.D., Allen, J.C., Stephenson, W.J., 2000. Shoreline erosion on Lake Hawea, New Zealand, caused by high lake levels and storm-wave runup. *Journal of Coastal Research*, 16, 346–356.

Kennedy, D.M., Paulik, R. and Dickson, M.E., 2011. Subaerial weathering versus wave processes in shore platform development: reappraising the Old Hat Island evidence. *Earth Surface Processes and Landforms*, *36*(5), 686-694.

Kline, S.W., Adams, P.N., Limber, P.W., 2014. The unsteady nature of sea cliff retreat due to mechanical abrasion, failure and comminution feedbacks. *Geomorphology*, *219*, 53-67.

Lantuit, H., Pollard, W.H., 2008. Fifty years of coastal erosion and retrogressive thaw slump activity on Herschel Island, southern Beaufort Sea, Yukon Territory, Canada. *Geomorphology*, *95*(1), 84-102.

Lee, E.M., 2008. Coastal cliff behaviour: Observations on the relationship between beach levels and recession rates. *Geomorphology*, *101*(4), 558-571.

Komar, P.D., 1985. Computer models of shoreline configuration: headland erosion and the graded beach revisited. In: Woldenberg, M.J. (Ed.), Models in Geomorphology. Allen
and Unwin, London.

Limber, P.W., Brad Murray, A., Adams, P.N. and Goldstein, E.B., 2014. Unraveling the dynamics that scale cross-shore headland relief on rocky coastlines: 1. Model development. *Journal of Geophysical Research: Earth Surface*, *119*(4), 854-873.

Limber, P.W. and Murray, A.B., 2014. Unraveling the dynamics that scale cross-shore headland relief on rocky coastlines: 2. Model predictions and initial tests. *Journal of Geophysical Research: Earth Surface*, *119*(4), 874-891.

Matsumoto, H., Dickson, M.E. and Masselink, G., 2017. Systematic analysis of rocky shore platform morphology at large spatial scale using LiDAR-derived digital elevation models. *Geomorphology*, *286*, 45-57.

May, V.J. and Heeps, C., 1985. The nature and rates of change on chalk coastlines. *Zeitschrift für Geomorphologie*, *57*, 81-94.

May, J.P., Tanner, W.F., 1973. The littoral power gradient and shoreline changes. In: Coates, D.R. (Ed.), Coastal Geomorphology. State Univ. New York, Binghamton.

Michaelsen, J., Haston, L., Davis, F.W., 1987. 400 years of central California precipitation variability reconstructed from tree-rings. *JAWRA Journal of the American Water Resources Association*, *23*(5), 809-818.

Mushkin, A., Katz, O., Crouvi, O., Alter, S.R. and Shemesh, R., 2016. Sediment contribution from Israel's coastal cliffs into the Nile's littoral cell and its significance to cliff-retreat mitigation efforts. *Engineering Geology*, *215*, 91-94.

Nicholls, R.J., Wong, P.P., Burkett, V.R., Codignotto, J.O., Hay, J.E., McLean, R.F., Ragoonaden, S., Woodroffe, C.D., 2007. Coastal systems and low-lying areas. In: Parry, M.L., Canziani, O.F., Palutikof, J.P., van der Linden, P.J., Hanson, C.E. (Eds.), Climate Change 2007: Impacts, Adaptation and Vulnerability. Contribution of Working Group II to the Fourth Assessment Report of the Intergovernmental Panel on Climate Change. Cambridge University Press, Cambridge, UK, 315–356.

Nunes, M., Ferreira, Ó., Loureiro, C. and Baily, B., 2011. Beach and cliff retreat induced by storm groups at Forte Novo, Algarve (Portugal). *Journal of Coastal Research*, (64), 795.

Obu, J., Lantuit, H., Grosse, G., Günther, F., Sachs, T., Helm, V. and Fritz, M., 2016. Coastal erosion and mass wasting along the Canadian Beaufort Sea based on annual airborne LiDAR elevation data. *Geomorphology*.

O'Reilly, W.C., Guza, R.T., 1991. Comparison of spectral refraction and refraction–diffraction wave models. *Journal of Waterway, Port, Coastal, and Ocean Engineering (ASCE)*, 117, 199-215.

O'Reilly, W.C., Guza, R.T., 1998. Assimilating coastal wave observations in regional swell predictions. Part I: inverse methods. *Journal of Physical Oceanography,* 28, 679-691.

O'Reilly, W.C., Olfe, C.B., Thomas, J., Seymour, R.J., Guza, R.T., 2016. The California coastal wave monitoring and prediction system. *Coastal Engineering*, *116*, 118-132.

Pawka, S.S., 1983. Island shadows in wave directional spectra, *Journal of Geophysical Ressearch*, 88(C4), 2579-2591.

Perry, T., 2000, January 16. Landslide Kills Woman as She Watches Husband Surf, *Los Angeles Times.*

Robinson, L.A., 1977. Marine erosive processes at the cliff foot. *Marine Geology*, *23*(3), 257-271.

Rosser, N.J., Lim, M., Petley, D. N. 2005. The use of terrestrial laser scanning for monitoring the process of hard rock coastal cliff erosion, Q. J. Eng. Geol. Hydrogeol., 35, 71–78.

Rosser, N., Lim, M., Petley, D., Dunning, S. and Allison, R., 2007. Patterns of precursory rockfall prior to slope failure. *Journal of geophysical research: earth surface*, *112*(F4).

Rosser, N.J., Brain, M.J., Petley, D.N., Lim, M. and Norman, E.C., 2013. Coastline retreat via progressive failure of rocky coastal cliffs. *Geology*, *41*(8), 939-942.

Ruggiero, P., Komar, P.D., McDougal, W.G., Marra, J.J., Beach, R.A., 2001. Wave runup, extreme water levels and the erosion of properties backing beaches. *Journal of Coastal Research,* 17, 407–419.

Sadler, P.M., Jerolmack, D.J., 2015. Scaling laws for aggradation, denudation and progradation rates: the case for time-scale invariance at sediment sources and sinks. *Geological Society, London, Special Publications*, *404*(1), 69-88.

Sallenger Jr, A.H., Krabill, W., Brock, J., Swift, R., Manizade, S., Stockdon, H., 2002. Sea-cliff erosion as a function of beach changes and extreme wave runup during the 1997–1998 El Niño. *Marine Geology*, *187*(3), 279-297.

Shih, S.M., Komar, P.D., Tillotson, K.J., McDougal, W.G., Ruggiero, P., 1994. Wave run-up and sea-cliff erosion. Coastal Engineering 1994 Proceedings, 24th International

Conference, American Society of Civil Engineers, 2170–2184.

Stephenson, W.J. and Kirk, R.M., 1996. Measuring erosion rates using the micro-erosion meter: 20 years of data from shore platforms, Kaikoura Peninsula, South Island, New Zealand. *Marine Geology*, *131*(3-4), 209-218.

Stockdon, H.F., Holman, R.A., Howd, P.A., Sallenger Jr., A.H., 2006. Empirical parameterization of setup, swash, and runup. *Coastal Engineering*, 53, 573–588.

Storlazzi, C.D., Griggs, G.B., 2000. Influence of El Niño-Southern Oscillation (ENSO) events on the evolution of central California's shoreline. *Geo logical Society of America Bulletin,* 112, 236–249.

Strolazzi, C., Willis, C., Griggs, G., 2000. Comparative impacts of the 1982-83 and 1997-98 El Niño winters on central California. *Journal of Coastal Research*, *16*, 1022-1036

Sunamura, T., 1976. Feedback relationship in wave erosion of laboratory rocky coast. *The Journal of Geology*, *84*(4), 427-437.

Sunamura, T., 1982. A wave tank experiment on the erosional mechanism at a cliff base.
Earth Surf. Process. Landf. 7, 333–343.

Sunamura, T., 1988. Projection of future coastal cliff recession under sea level rise induced by the green house effect: Nii-jima Island, Japan. *Trans. Japan Geomorph. Union*, *9*, 17-33.

Sunamura, T., 1992. Geomorphology of Rocky Coasts. John Wiley and Sons, New York, 302p.

Thomas, M.A., Loague, K., 2014. Devil's Slide: An evolving feature of California's coastal landscape. *Environmental & Engineering Geoscience*, *20*(1), 45-65.

Trenhaile, A.S., 1987. The Geomorphology of Rock Coasts. Oxford University Press, New York. 384p.

Trenhaile, A.S., 2010. Modeling cohesive clay coast evolution and response to climate change. *Marine Geology*, *277*(1), 11-20.

Trenhaile, A.S., 2014. Climate change and the impact on rocky coasts. In: Kennedy, D.A., Stephenson, W.J., Naylor, L.A. (Eds.), Rock Coast Geomorphology: A Global Synthesis. Geol. Geological Society of London Memoirs, 40, 7–17.

Trenhaile, A.S., 2016. Rocky coasts—their role as depositional environments. *Earth-Science Reviews*, *159*,1-13.

U.S. Army Corps of Engineers, 1971. *National Shoreline Study California Regional Inventory,* San Francisco: USACE South Pacific Division. 106p.

Vann Jones, E., Rosser, N.J., Brain, M.J. and Petley, D.N., 2015. Quantifying the environmental controls on erosion of a hard rock cliff. *Marine Geology*, *363*, 230-242.

Vaughan, T.W., 1932. Rate of sea cliff recession on the property of the Scripps Institution of Oceanography at La Jolla, California. *Science*, *75*, 250.

Williams, A.T. and Davies, P., 1987. Rates and mechanisms of coastal cliff erosion in Lower Lias rocks. In *Coastal sediments* (1855-1870). ASCE.

Young, A.P., Ashford, S.A., 2006. Application of airborne LIDAR for seacliff volumetric change and beach-sediment budget contributions*. Journal of Coastal Research* 22, 307-318.

Young, A.P., Flick, R.E., Gutierrez, R., Guza, R.T., 2009a. Comparison of short-term seacliff retreat measurement methods in Del Mar, CA. *Geomorphology* 112, 318-323.

Young, A.P., Guza, R.T., Flick, R.E., O'Reilly, W.C., Gutierrez, R., 2009b. Rain, waves, and short-term seacliff evolution. *Marine Geology,* 267, 1-7.

Young, A.P., Raymond, J.H., Sorenson, J., Johnstone, E.A., Driscoll, N.W., Flick, R.E., Guza, R.T., 2010a. Coarse Sediment Yields from Seacliff Erosion in the Oceanside Littoral Cell. *Journal of Coastal Research,* 26, 580-585.

Young, A.P., Olsen, M.J., Driscoll, N., Flick, R.E., Gutierrez, R., Guza, R.T., Johnstone, E., Kuester, F., 2010b. Comparison of airborne and terrestrial LIDAR estimates of seacliff erosion in southern California. *Photogrammetric Engineering and Remote Sensing,* 76, 421-427.

Young, A.P., Guza, R.T., O'Reilly, W.C., Flick, R.E., Gutierrez, R., 2011. Short-term retreat statistics of a slowly eroding coastal cliff. *Natural Hazards and Earth System Sciences,* 11, 205-217.

Young, A.P., 2015. Recent deep-seated coastal landsliding at San Onofre State Beach, California. *Geomorphology*, *228*, 200-212.

Young, A.P., Guza, R.T., O'reilly, W.C., Burvingt, O. and Flick, R.E., 2016. Observations of coastal cliff base waves, sand levels, and cliff top shaking. *Earth Surface Processes and Landforms*, *41*(11), 1564-1573.

Fig. 1. a) Map of California's coastal cliffs/rocky shoreline and the LiDAR study area spanning 1100 km of shoreline. LiDAR data coverage was incomplete in some regions (boxes) resulting in 595 km of cliffed shoreline for analysis. Rain (circles) and tide (triangle) gauges used for this study were located alongshore in the study area. Example photos of representative California coastal cliff settings: b) low relief cliffs fronted by a beach in Goleta, c) high relief cliff at Torrey Pines, La Jolla and d) cliff top development, sea caves, and crenulated cliff line in Sunset Cliffs, San Diego. Photographs used with permission, ©2002-2017 Kenneth and Gabrielle Adelman, California Coastal Records Project www.Californiacoastline.org.

Fig. 2. Interpretations of idealized cliff changes using the different retreat and erosion estimates.

Fig. 3. Alongshore comparison of (a) coastal setting and classification, (b) cliff or coastal slope height, (c) total water level index (hours above 2.5 m NAVD88), (d) interpolated study period total precipitation, (e) Schmidt hammer rebound metrics (within 1 km of compartment location) and (f) coastline reference map with hashes at 200 km intervals. Lower rebound metrics correspond to weaker rocks.

Fig. 4. Alongshore comparison of (a) historical cliff top retreat (b) recent cliff top retreat (c) recent net cliff face retreat, (d) recent volumetric cliff change, (e) cliff top hazard index, and (f) coastline reference map with hashes at 200 km intervals.

Positive cliff top hazard index numbers indicate higher hazard and slope steepening. Numbers show cliff retreat hot spots and high cliff top hazard locations at (1) San Onofre State Beach, (2) Portuguese Bend, (3) Palos Verdes, (4) Big Sur, (5) Martins Beach, (6) Daly City, (7) Double Point, and (8) Point Reyes. The net cliff volume change (d) at about km 1000 extends beyond the plot (dashed line) to -527 $m^3/m/yr$.

Fig. 5. Examples of significant coastal cliff changes at (a) Point Reyes National Seashore, (b) Martin's Beach, (c) Daly City and Pacifica, (d) Portuguese Bend, and (e) Palos Verdes. Inland lines in panels c and d show LiDAR analysis boundary, indicating possible additional cliff changes occurring further inland. See Fig. 4 for mapped locations.

Fig. 6. Cumulative distributions of recent 1998 to 2009-2010 (a) cliff face retreat rate for armored, all unarmored, unarmored with/out beaches, and all cliffs, (b) cliff face retreat rate (erosion normalized by cliff height) for cliffs separated by cliff height (colors), and (c) cliff face erosion rate for cliffs separated by cliff height (colors). For panels b & c, only binned height ranges with at least 1000 observations are shown.

Fig. 7. Binned (0.1 m) distribution of historical and recent cliff retreat rates. Negative values indicate landward retreat.

Fig. 8. Comparison of (a) historical (1929-1934 to 1998/2002) cliff top and recent (1998/2002 to 2009-2010) cliff top retreat, (b) historical cliff top and recent cliff face retreat, and (c) recent cliff top and recent cliff face retreat. Color bars represent grid point density. (d-f) Correlations of retreat rates of corresponding top panels (a-c) for alongshore compartments with minimum historical or recent retreat rate magnitudes.

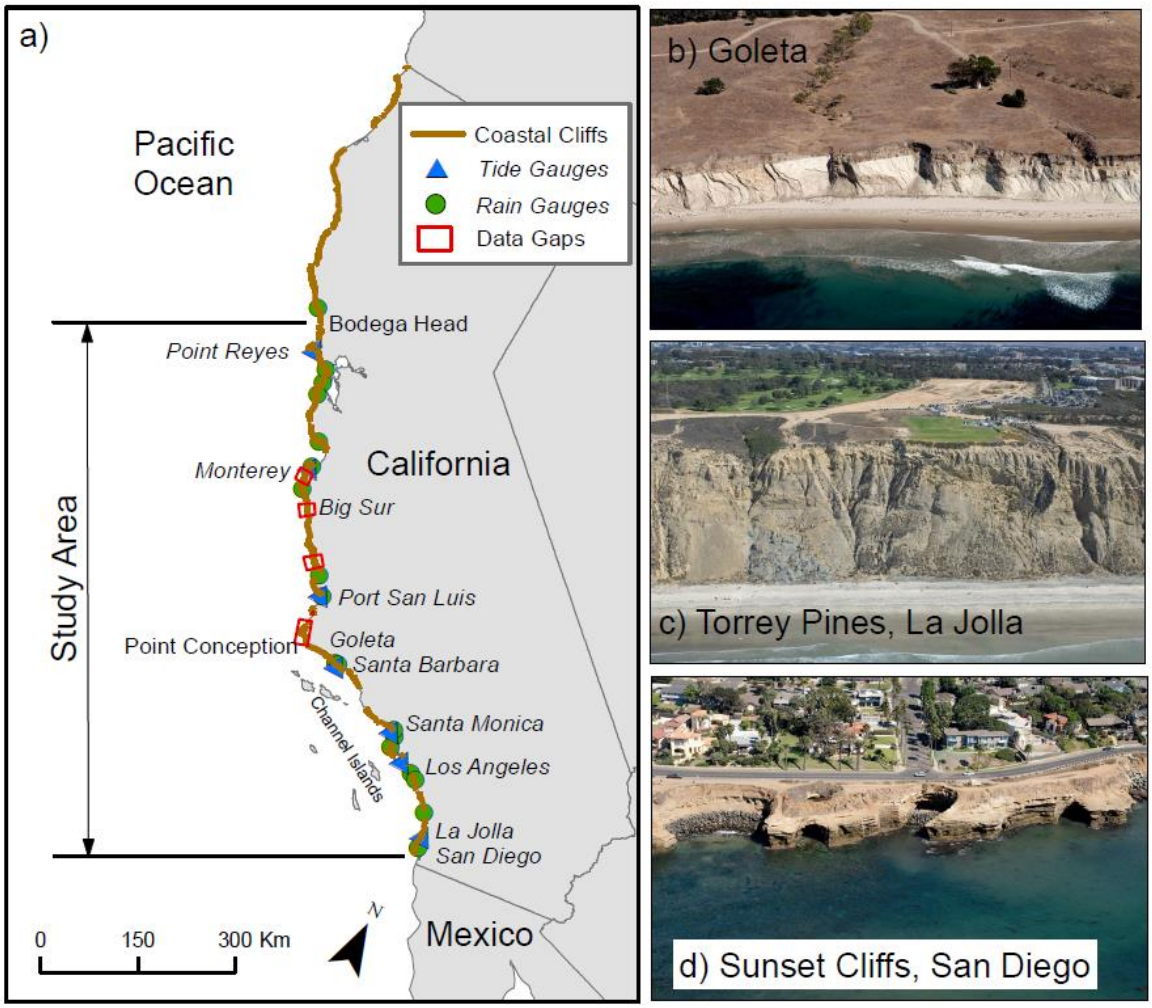
a)
Pacific Ocean
Coastal Cliffs
Tide Gauges
Rain Gauges
Data Gaps
Bodega Head
Point Reyes
Monterey
California
Big Sur
Port San Luis
Point Conception
Goleta
Santa Barbara
Channel Islands
Santa Monica
Los Angeles
La Jolla
San Diego
Study Area
0
150
300 Km
N
Mexico
b) Goleta
c) Torrey Pines, La Jolla
d) Sunset Cliffs, San Diego

Figure 1

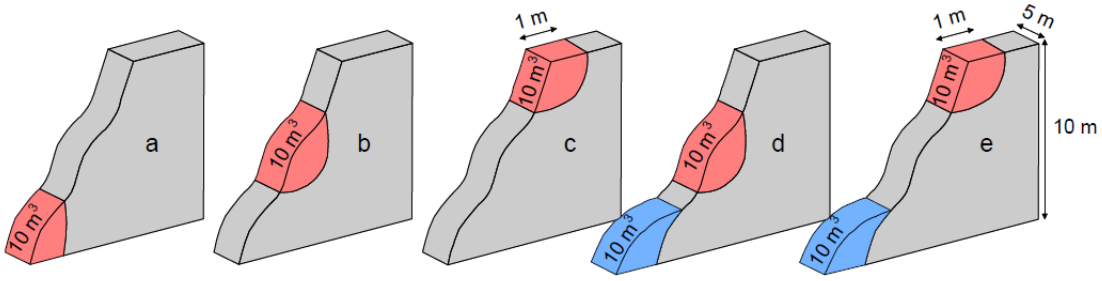

Erosion
Talus Deposit

Cliff Change Measurements

	a	b	c	d	e
Cliff Retreat (m)					
Top =	0.0	0.0	-1.0	0.0	-1.0
Face (-) =	-0.2	-0.2	-0.2	-0.2	-0.2
Face (+) =	0.0	0.0	0.0	+0.2	+0.2
Face (Net) =	-0.2	-0.2	-0.2	0.0	0.0
Cliff Erosion (m^3/m)					
Volume (-) =	-2.0	-2.0	-2.0	-2.0	-2.0
Volume (+) =	0.0	0.0	0.0	+2.0	+2.0
Volume (Net) =	-2.0	-2.0	-2.0	0.0	0.0

Figure 2

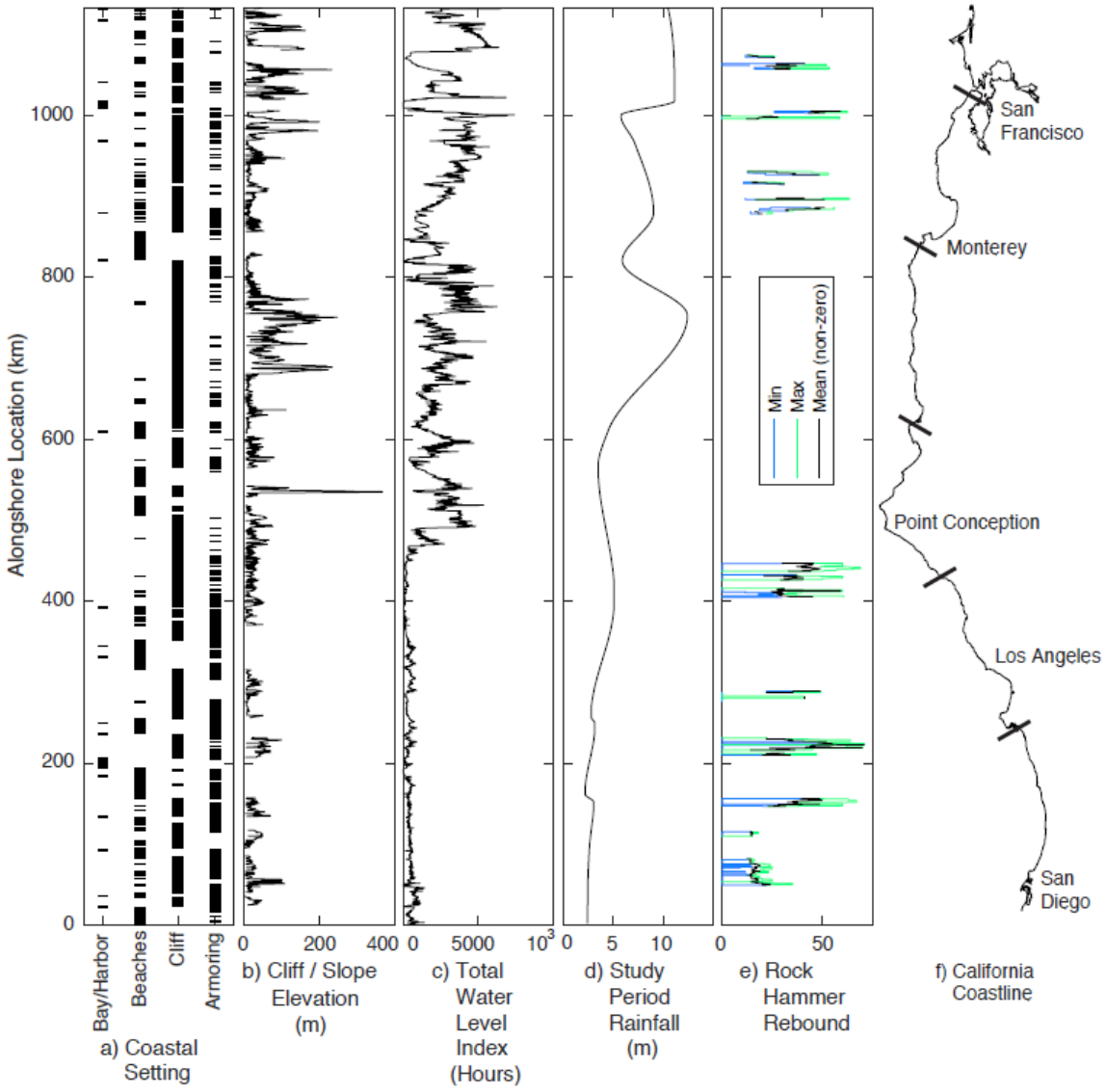
Alongshore Location (km)
0
200
400
600
800
1000
Bay/Harbor
Beaches
Cliff
Armoring
a) Coastal Setting
0
200
400
b) Cliff / Slope Elevation (m)
0
5000
10^3
c) Total Water Level Index (Hours)
0
5
10
d) Study Period Rainfall (m)
0
50
Min
Max
Mean (non-zero)
e) Rock Hammer Rebound
San Francisco
Monterey
Point Conception
Los Angeles
San Diego
f) California Coastline

Figure 3

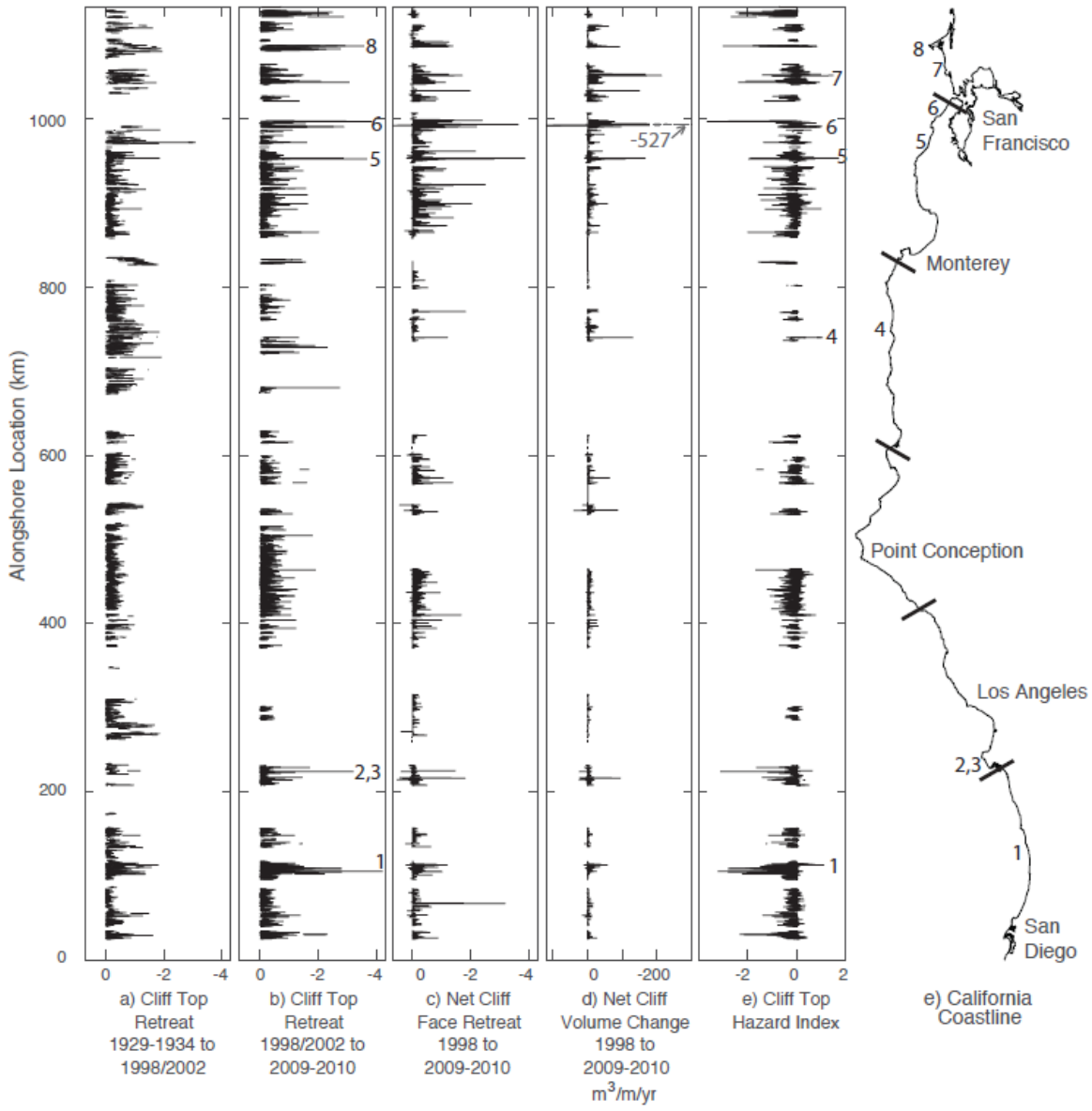
Alongshore Location (km)
0
200
400
600
800
1000
a) Cliff Top Retreat 1929-1934 to 1998/2002
b) Cliff Top Retreat 1998/2002 to 2009-2010
c) Net Cliff Face Retreat 1998 to 2009-2010
d) Net Cliff Volume Change 1998 to 2009-2010 m3/m/yr
e) Cliff Top Hazard Index
-527
8
7
6
5
4
2,3
1
San Francisco
Monterey
Point Conception
Los Angeles
San Diego
e) California Coastline

Figure 4

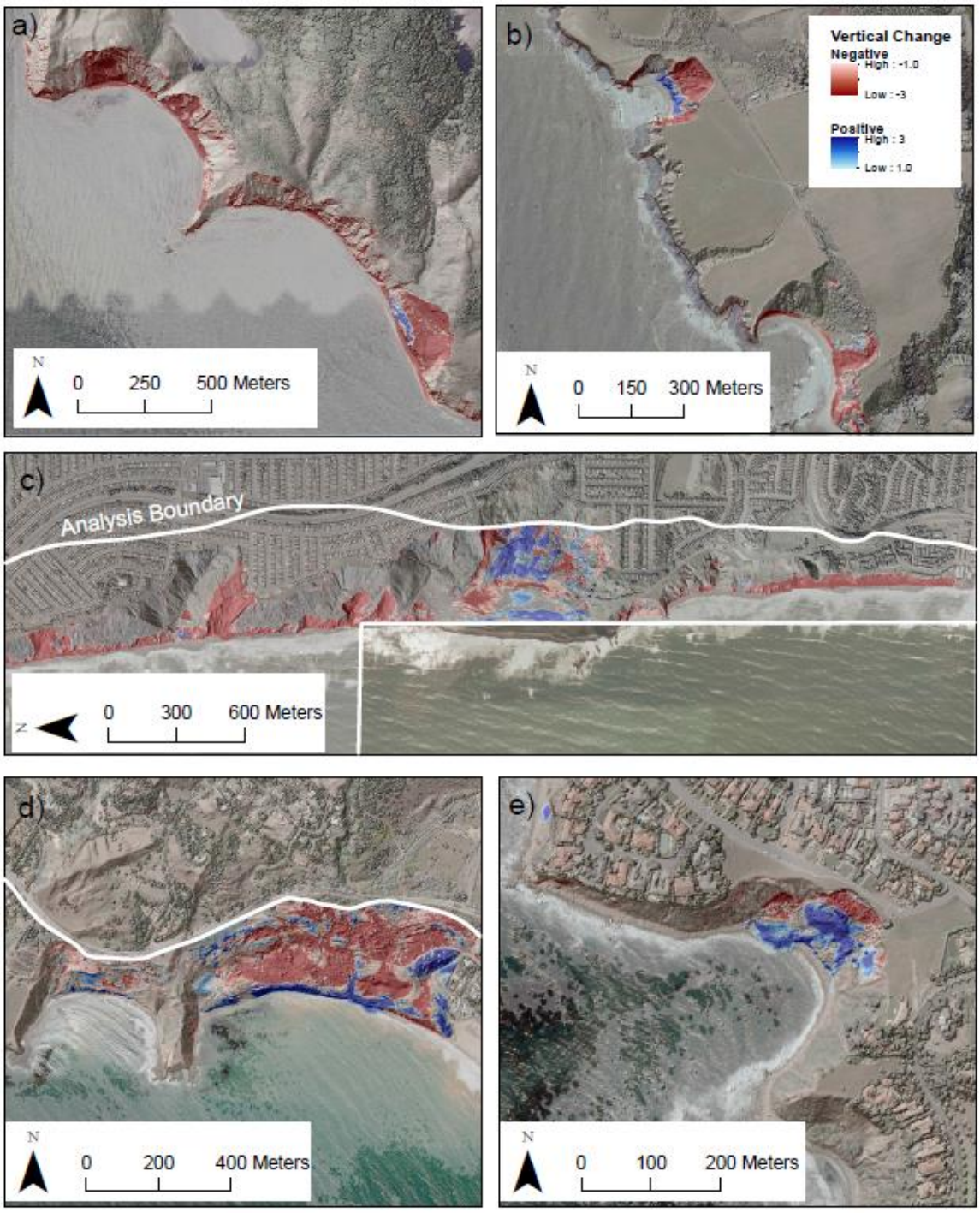
a)
N
0 250 500 Meters
b)
Vertical Change
Negative
High : -1.0
Low : -3
Positive
High : 3
Low : 1.0
N
0 150 300 Meters
c)
Analysis Boundary
N
0 300 600 Meters
d)
N
0 200 400 Meters
e)
N
0 100 200 Meters

Figure 5

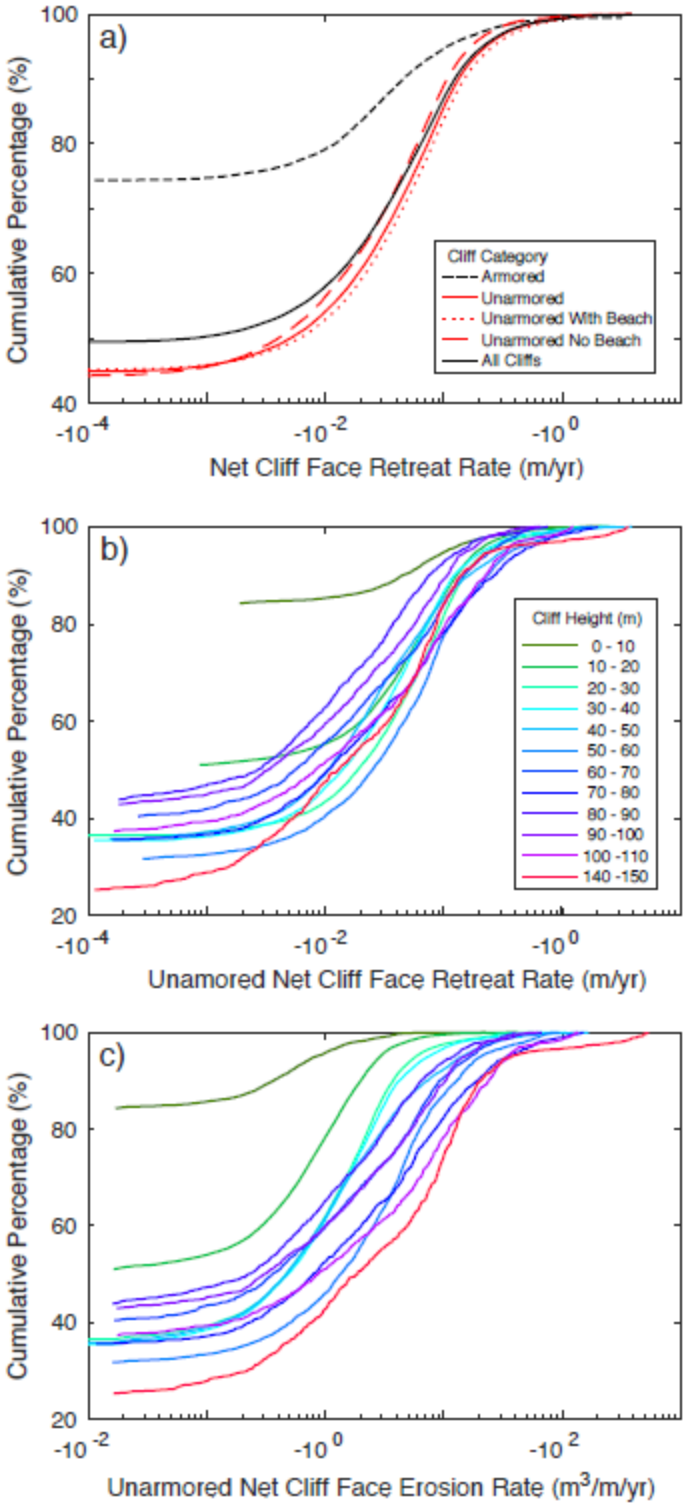
a)
Cumulative Percentage (%)
100
80
60
40
-10^-4
-10^-2
-10^0
Net Cliff Face Retreat Rate (m/yr)
Cliff Category
Armored
Unarmored
Unarmored With Beach
Unarmored No Beach
All Cliffs
b)
Cumulative Percentage (%)
100
80
60
40
20
-10^-4
-10^-2
-10^0
Unamored Net Cliff Face Retreat Rate (m/yr)
Cliff Height (m)
0 - 10
10 - 20
20 - 30
30 - 40
40 - 50
50 - 60
60 - 70
70 - 80
80 - 90
90 -100
100 -110
140 -150
c)
Cumulative Percentage (%)
100
80
60
40
20
-10^-2
-10^0
-10^2
Unarmored Net Cliff Face Erosion Rate (m^3/m/yr)

Figure 6

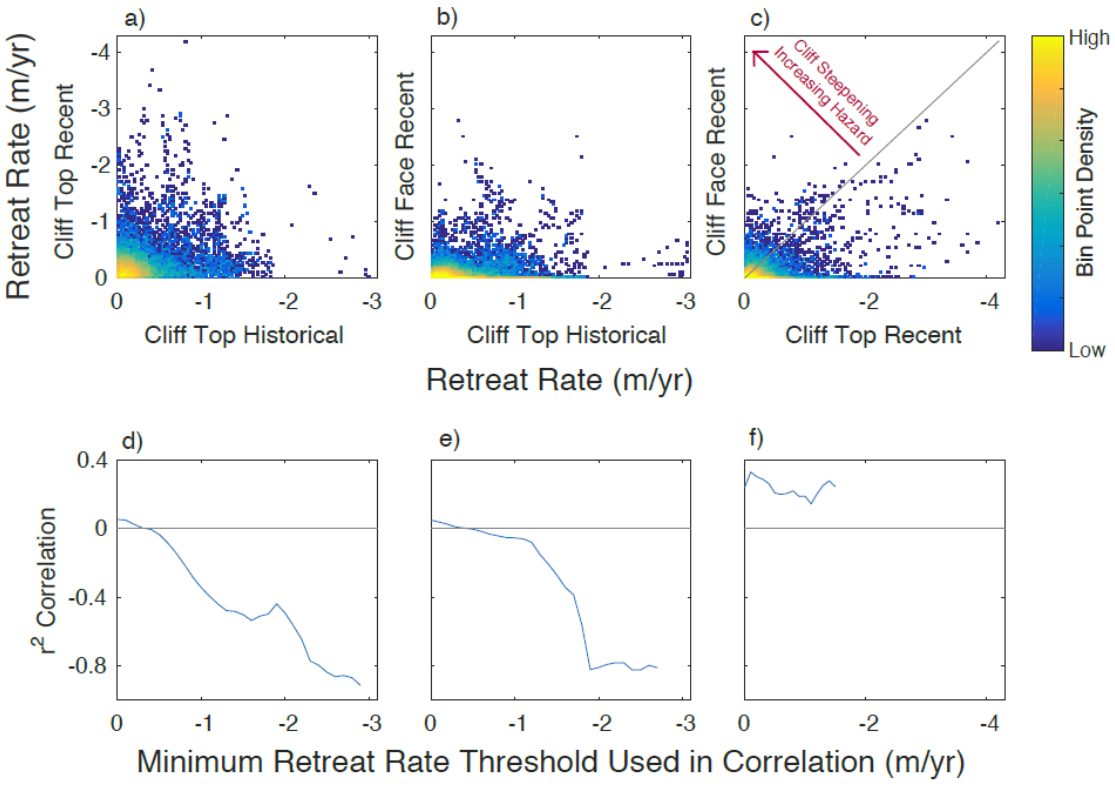
a)
b)
c)
Retreat Rate (m/yr)
Cliff Top Recent
Cliff Face Recent
Cliff Face Recent
Cliff Top Historical
Cliff Top Historical
Cliff Top Recent
Cliff Steepening
Increasing Hazard
High
Bin Point Density
Low
Retreat Rate (m/yr)
d)
e)
f)
r2 Correlation
Minimum Retreat Rate Threshold Used in Correlation (m/yr)

Figure 7

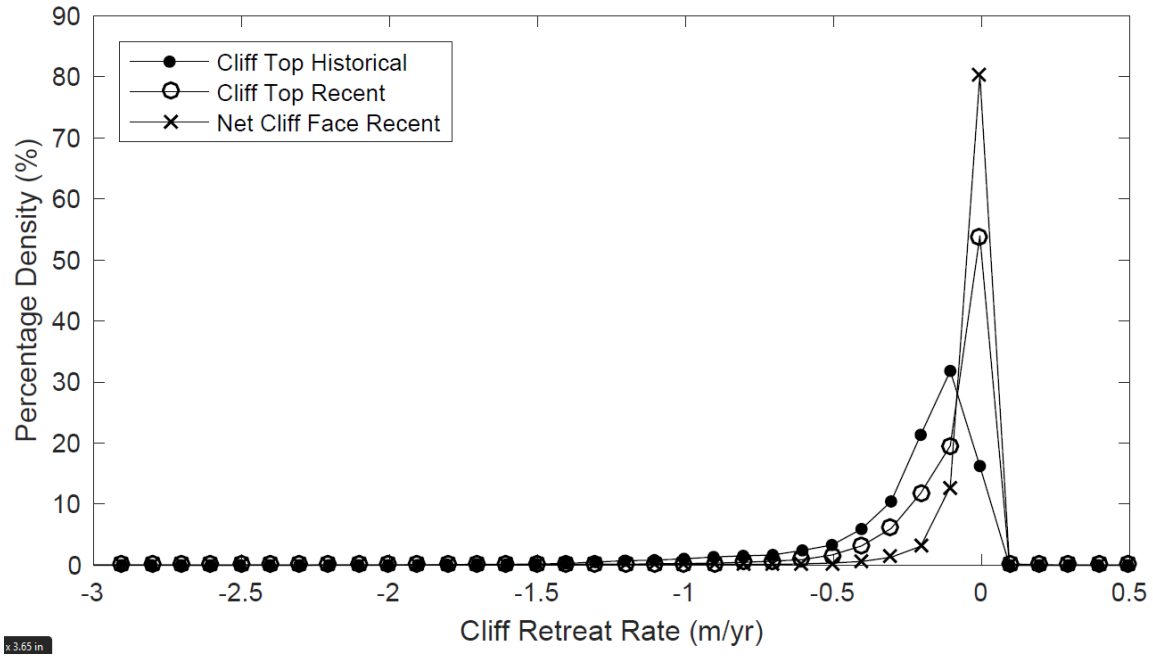
Cliff Top Historical
Cliff Top Recent
Net Cliff Face Recent
Percentage Density (%)
Cliff Retreat Rate (m/yr)
90
80
70
60
50
40
30
20
10
0
-3
-2.5
-2
-1.5
-1
-0.5
0
0.5

Figure 8

Table 1. 2009-2010 lidar coverage and survey dates (Fugro, 2011)

South End	North End	Survey Date	Analysis Time Span (years, 1998 to 2009-2010)*
Border	La Jolla Shores	November 2009	11.6
La Jolla Shores	Dana Point Harbor	October 2009	11.5
Dana Point Harbor	Seal Beach	October 2009	11.5
Seal Beach	Point Dume	October 2009	11.6
Point Dume	Carpenteria	November 2009	11.6
Carpenteria	El Capitan	November 2009	11.6
El Capitan	Point Conception	November 2009	11.6
Point Conception	Oceano	November 2009	11.6
Oceano	Harmony	November 2009, May 2010	11.6
Harmony	Ragged Point	November 2009	11.6
Ragged Point	Point Sur	November 2009, May 2010	11.7
Point Sur	Moss Landing	May 2010, June 2010, October 2010	12.1
Moss Landing	Ano Neuevo	June 2010, September 2010, October 2010	12.2
Ano Neuevo	Pacfica	June 2010, September 2010, November 2010	12.2
Pacifica	Golden Gate	June 2010, October 2010, November 2010	12.2
Golden Gate	Tomales Bay	September 2010, November 2010	12.4
Tomales Bay	Sea Ranch	September 2010, November 2010	12.4

*Longest Date Range

Table 2. Coastal setting, cliff change, and cliff top hazard statistics by county

County	Length in Study Area (km)	Classification (%) Armored	Beach	Cliff & Beach	Cliff/ Rocky	Bay / Harbor	Mean Wave Impact Index *	Mean Rock Rebound Value *	Mean Recent Cliff Top Retreat (m/yr)	Mean Recent Cliff Face Retreat (m/yr)	Length of Cliff Top Evaluated (km)	Length of Cliff Face Evaluated (km)	Cliff Top Hazard Index Mean of Positive Values Mean	Cliff Top Hazard Index Mean of Positive Values Values	Percent Positive Values (%)
Sonoma	7	2	42	25	26	7	2538	NaN	-0.32	-0.01	1	6	-0.31	0.005	10
Marin	111	3	21	42	33	3	2872	28	-0.21	-0.07	21	75	-0.06	0.11	54
San Francisco	19	23	26	23	23	28	2375	32	-1.08	-0.16	0	9	-0.82	0.12	11
San Mateo	82	10	13	52	32	3	3951	27	-0.16	-0.09	23	74	-0.05	0.09	34
Santa Cruz	62	24	18	49	33	0	1854	34	-0.09	-0.04	21	57	-0.05	0.04	28
Monterey	167	4	20	13	66	1	2547	NaN	-0.13	-0.01	15	63	-0.17	0.04	23
San Luis Obispo	140	8	24	21	53	1	1963	NaN	-0.04	-0.04	24	41	-0.01	0.05	62
Santa Barbara	176	12	22	70	8	0	1317	37	-0.11	-0.05	66	102	-0.05	0.06	42
Ventura	67	55	52	31	15	2	399	NaN	NaN	0.00	0	13	NaN	NaN	NaN
Los Angeles	117	27	21	51	13	14	325	38	-0.09	-0.02	18	59	-0.07	0.02	22
Orange	67	42	54	35	8	4	380	37	-0.09	-0.01	6	22	-0.07	0.01	25
San Diego	120	31	40	45	12	3	558	16	-0.14	-0.02	40	74	-0.12	0.03	15
All	1,133	18	27	40	30	3	1683	18	-0.12	-0.04	236	595	-0.07	0.05	33

* Compartment means for wave and rock metrics shown in Figure 2

Table 3. Summary of cliff change statistics

	Maximum Erosion or Landward Movement	Maximum Accretion or Seaward Movment	Mean	Standard Deviation	Percentage of NonZero Compartement Observations (%)
Cliff Volume Change Rate (m^3/m/yr) 1998 to 2009-2010					
Negative (erosion)	-527	0	-1.95	9.66	44
Positive (accretion)	0	136	0.17	2.27	4
Net	-527	128	-1.78	9.56	45
Cliff Face Retreat Rate (m/yr) 1998 to 2009-2010					
Negative (erosion)	-4	0	-0.045	0.141	44
Positive (accretion)	0	1.12	0.0023	0.028	4
Net	-3.8	0.67	-0.042	0.14	45
Cliff Top Retreat Rate (m/yr) 1998/2002 to 2009-2010					
Negative (landward)	-4.2	0	-0.12	0.27	55
Cliff Top Retreat Rate (m/yr) 1929-1934 to1998/2002					
Negative (landward)	-3.1	0	-0.25	0.28	99